Spectral Analysis Algorithms for the Laser Velocimeter: A Comparative Study

W. A. Bell*
Lockheed-Georgia Company, Marietta, Georgia

Conventional methods of computing spectra require constant sampling rates and therefore must be modified to accommodate the randomly sampled data from the laser velocimeter. Four approaches that provide estimates of the power spectra from randomly sampled data are evaluated with respect to accuracy and computational speed. Simulated data of varying spectral content are used as input. An estimate of the correlation function that resolves the random time distribution into equidistant time intervals provides the best compromise between computational speed and accuracy for laser velocimeter data.

Introduction

FOURIER analysis of fluctuating signals is an important part of digital signal processing. For data sampled at constant rates, the methods for spectral and correlation analyses have been extensively studied and widely used. When the data are randomly sampled, however, relatively new methods for spectral and correlation estimates must be employed.

A practical need for such estimates occurs when data are obtained from the laser velocimeter (LV). With this instrument an interference pattern is formed by two intersecting laser beams. The surrounding fluid is seeded with particles and, assuming that the particles respond exactly to the flow conditions, the fluid velocity is determined from the transit time across the interference pattern. Since the particles cross the measurement volume at irregular time intervals, conventional spectral estimates based on constant sampling rates must be modified.

Background

In time series analysis, two methods are generally used to obtain the spectrum.[1,2] The first is based on the Wiener-Khinchine theorem, which relates the power spectrum to the Fourier transform of the correlation function. When the data are sampled at a constant rate, the correlation function is computed first, a window function is then applied to minimize the effects of finite sampling times, and the Fourier transform is taken. This approach is known as the Blackman-Tukey algorithm. For the randomly sampled LV data, modifications of this algorithm have been derived in Refs. 3-7. In the second approach, a discrete Fourier transform of the digitized signal is applied. After the data are sampled over a given time interval and a window function employed, the Fourier transform is taken. The resulting complex number is multiplied by either the complex conjugate of itself to give the periodogram, which is proportional to the auto power spectrum, or another transformed signal to yield the cross spectrum. The resulting spectra are obtained for a series of time intervals and then averaged over a specified number of blocks to increase accuracy. When the data are sampled at a constant rate, the fast Fourier transform (FFT) can be used to significantly reduce the computation times. The FFT cannot be used for the randomly sampled LV data, however. Consequently spectral estimates for randomly sampled data take longer to compute for a given number of samples and frequency resolution. Estimates applicable to LV measurements are presented in Refs. 8-11.

For both periodic and random sampling, two types of errors arise—bias and variance. Bias is a systematic error, such as aliasing, which distorts the resulting spectrum. Estimates for randomly sampled data are, in principle, free from aliasing. Variance results from random errors and generally decreases with increasing sample size. The estimate is consistent if the variance approaches zero as the number of samples becomes infinite.

This investigation compares the existing approaches for spectral estimation from randomly sampled data from a computational point of view. First, the effect of random sampling on the variance of the spectral estimates is investigated analytically and then tested numerically using simulated random signals. Then a comparison between the spectra obtained with correlation and periodogram estimates are made to determine the relative computation times and accuracies.

Numerical Procedure

As pointed out in the last section, two methods are generally used to obtain the power spectrum from digital data. The first consists of taking the discrete Fourier transform of the digitized correlation function to obtain the power spectrum, and the second involves taking the discrete Fourier transform of the digital signal. Obtaining exact results with either of these two methods involves the evaluation of infinite integrals. In digital data analysis these integrals are replaced by finite sums or estimates. The estimates presented in this section give unbiased, consistent results as the number of samples or the sampling rate becomes infinite. These estimates will be evaluated with respect to the number of computations required to obtain the power spectrum from a given data set and the numerical errors arising from the finite sampling rates and times.

Power Spectra from Correlation Functions

Before the development of the FFT, power spectral data were obtained by first computing the correlation function. The auto correlation function R_{xx} of a signal $x(t)$ is given by

$$R_{xx}(\tau) = \lim_{T\to\infty} \frac{1}{T-\tau} \int_{-T/2}^{T/2} x(t)x(t+\tau)\,\mathrm{d}\tau \qquad (1)$$

where τ is the time lag and T the total sampling time.

Presented as Paper 81-1196 at the AIAA 14th Fluid and Plasma Dynamics Conference, Palo Alto, Calif., June 23-25, 1981; submitted July 13, 1981; revision received Aug. 27, 1982. Copyright © American Institute of Aeronautics and Astronautics, Inc., 1982. All rights reserved.

*Specialist Engineer, Electronics Laboratory Department. Member AIAA.

The spectrum can then be obtained from the Wiener-Khinchine theorem

$$S_{xx}(\omega) = \int_{-\infty}^{\infty} R_{xx}(\tau)\exp(i\omega\tau)\,\mathrm{d}\tau \qquad (2)$$

In Refs. 4-6, estimates are obtained by combining Eqs. (1) and (2) and discretizing to give

$$\hat{S}_{xx}(\omega) = \frac{2T}{N^2}\sum_{k>r}^{N} x_k x_r D(t_k - t_r)\cos[\omega(t_k - t_r)] \qquad (3)$$

where N is the number of samples taken over the time T. The window function D is used to limit the maximum time lag by having a value of unity at a zero time lag and decreasing to zero after the maximum time lag. For periodic sampling, the window function significantly affects the side lobe structure of the spectra.

As pointed out in Refs. 12 and 13, Eq. (3) does not include the effects of velocity biasing when the variable x is taken to be the velocity measured by the LV. Assuming that angle effects have been minimized by frequency shifting with a Bragg cell,[14] Ref. 13 provides an unbiased estimate of the correlation function, by letting

$$x_k = u_k \Delta t_k / \sqrt{\Sigma \Delta t_k \Delta t_r}$$

and

$$x_r = u_r \Delta t_r / \sqrt{\Sigma \Delta t_k \Delta t_r}$$

where u_k and u_r are the velocity fluctuations and Δt the residence time of the particle in the measurement volume. The subsequent discussions assume that the velocity bias has been accounted for. The main thrust of this paper can now deal with the numerical efficiency and accuracy of the respective spectral estimates.

As shown in Table 1 the number of operations required to produce a spectrum is comparatively large. There is a total of $3m^2N/2$ multiplications and $m^2N/2$ cosine function evaluations for a total of $2m^2N$ operations where m is the number of frequencies in the spectrum.

This estimate has been shown to be unbiased and consistent as the sampling time T becomes infinite.[6] However, for finite sampling times the sums in Eq. (3) contain more terms with short time lags than with long ones, the number of terms generally decreasing with lag times. This phenomenon is caused by neglecting the term $T-\tau$ in Eq. (1), which is a good approximation if the total sampling time is much larger than the maximum time lag. Mayo[4] points out that the $T-\tau$ term is an important consideration in segmented data techniques where T and τ are of the same order. For example, if the sampling is periodic and T is twice the maximum time lag, then the spectrum derived from Eq. (3) with a rectangular window function is equivalent to the spectrum obtained with a Bartlett window when this term is neglected.[7] This window leads to a relatively large ratio of side lobe to signal, which is generally unsatisfactory.

Table 1 Approximate number of computations required for spectral analysis from random data

Method	No. of computations[a]
Group A: Random times used	
1) Correlation method	$2N^2M$
2) Periodogram approach	NM
Group B: Random times resolved into equidistant intervals	
3) Correlation method	$MN/2$
4) Periodogram approach	$N\log_2 M$

[a] M = number of points in frequency domain. N = number of samples taken in time domain.

Gaster and Roberts[6] show that the expression for the expected error resulting in the spectrum obtained from Eq. (3) is approximately

$$e = \sqrt{\frac{3\tau_m \nu}{N}}\left[S_{xx}(\omega) + \frac{\sigma^2}{2\pi\nu}\right] \qquad (4a)$$

where σ is the standard deviation of the signal, τ_m the maximum lag time, and ν the sampling rate. This expression does not account for the effect of the $T-\tau$ term in Eq. (1) and therefore is an optimistic error estimate for blocked data. In the cases considered using Eq. (3) in Refs. 4-6, T is much larger than τ so Eq. (3) provides a reasonable estimate.

A much faster approach for computing the spectra is to calculate the correlation function first from Eq. (1). To do so, the time domain must be divided into equidistant slots so that Eq. (2) can be used to obtain the spectrum. The estimator for the autocorrelation is given as[3,4]

$$\hat{R}_{xx}(r) = \sum_{k=1}^{N} x_k x_{k+r} \Big/ H(r) \qquad (5)$$

where $H(r)$ is the number of lagged products in the lagged time slot r and arises from the $T-\tau$ term in the denominator of Eq. (1). A similar expression can be derived for the cross correlation. With Eq. (5) the maximum time lag is divided into N equidistant time intervals such that

$$\left| \frac{t_{k+r} - t_k}{\Delta\tau} - r \right| \le 0.5$$

where $t_{k+r} - t_k$ is the exact time between lagged products. Thus, some error in time is introduced in order to increase speed. The effects of this error on the spectrum has been analyzed in Ref. 7, which provides expressions describing its effect on the spectrum.

To provide further insight into this error, an alternate equation can be obtained by expanding the expression for the lagged signal in a Taylor series about the kth interval to obtain

$$x(t+\tau+e(\tau)) = x(t+\tau) + e(\tau)\dot{x}(t+\tau) + \mathcal{O}(e^2)$$

Thus from Eq. (1),

$$R_{xx}e(\tau) \simeq R_{xx}(\tau) + e(\tau)R_{x\dot{x}}(\tau) \qquad (4b)$$

where $e(\tau)$ is the deviation of the kth time lag from $k\Delta t$, $\dot{x}$ the derivative of x with respect to the time lag, and $R_{xx}(k)$ the autocorrelation function given by Eq. (1). The term $eR_{x\dot{x}}$ represents the bias in the correlation function (and thus in the spectrum) arising from the time approximation. Increasing the time variation or the deviation of the time approximation increases the bias. The effects of this term are evident in the spectra presented in the results section.

As shown by Table 1, R_{xx} computed from Eq. (5) requires significantly fewer arithmetic operations. Only one multiplication and one addition are required per lagged time product, and so the number of operations is reduced by a factor of $4m$ over the number required in Eq. (3). Also, the cosine function required in Eq. (3) need not be computed, reducing computer time even more. Finally, since equidistant time intervals are used, the FFT can be applied to compute the spectrum from the correlation function.

Spectral Estimates from Periodograms

Another method for obtaining the power spectrum of a signal is from its Fourier transform, referred to in Ref. 9 as the direct approach. Basically, it involves the discretization of the integral in the equation

$$X(\omega)=\int_{-\infty}^{\infty} x(t)\exp(i\omega t)\,dt \tag{6}$$

to obtain the estimate

$$\hat{X}(\omega)=\frac{\sqrt{T}}{N}\sum_k x_k D_k \exp(i\omega t_k) \tag{7}$$

where D_k is a window function and XX^* is the periodogram.

The following expressions then yield the auto and cross-power spectra, respectively:

$$S_{xx}=XX^* \tag{8}$$

and

$$S_{xy}=X^*Y$$

The estimate given by Eq. (7) is not consistent.[9] To obtain consistency and avoid large errors in the spectrum, the summation in Eq. (7) must be divided into several sums, each sum applying to a block of data taken over a fixed time interval. The resulting spectra are then averaged. For randomly sampled data, the number of arithmetic operations with this estimate is over twice that required in the slotted correlation method. Computation times are further increased because the complex exponential function must now be computed to obtain the periodogram.

Numerically the periodogram estimate suffers from a serious drawback for randomly sampled processes. Depending on the sampling distribution and spectral shape, numerical noise develops and is reflected in the spectrum. This noise is related to the side lobes appearing in the spectra of periodically sampled data. With random sampling, these lobes produce an apparent white noise on the spectrum as shown by Jones.[16] To investigate this phenomenon further, Eq. (7) can be rewritten as

$$\hat{X}(\omega)=\frac{\sqrt{T}}{N}\sum_{k=1}^{N} x(\xi_k)D(\xi_k)\exp(i\omega\xi_k) \tag{9}$$

where

$$(k-\tfrac{1}{2})\Delta t \le \xi_k \le (k+\tfrac{1}{2})\Delta t$$

and all k slots have at least one sample.

For periodic sampling, $\xi_k = k\Delta t$ whereas for random sampling

$$\xi_k = k\Delta t + \epsilon_k \Delta t$$

where ϵ_k is the deviation of the sampling time from the periodic sampling rate at the kth interval. Expanding x_k, D_k, and $\exp(i\omega t_k)$ in a Taylor series about $k\Delta t$ gives

$$x(k\Delta t+\epsilon_k\Delta t)=x(k\Delta t)+\epsilon_k\dot{x}(k\Delta t)\Delta t+\mathcal{O}(\epsilon_k^2)$$

$$D(k\Delta t+\epsilon_k\Delta t)=D(k\Delta t)+\epsilon_k D(k\Delta t)\Delta t+\mathcal{O}(\epsilon_k^2)$$

$$\exp[i\omega(k\Delta t+\epsilon_k\Delta t)]=\exp(i\omega k\Delta t)(1+i\omega\epsilon_k\Delta t)+\mathcal{O}(\epsilon_k^2)$$

Then Eq. (9) becomes

$$X(\omega)=X_p(\omega)+e_X(\omega)+\mathcal{O}[e_X^2(\omega)] \tag{10}$$

where $X_p(\omega)$ is the value obtained with periodic sampling. The term

$$e_X(\omega)=\frac{\sqrt{T}}{N}\sum_{k=1}^{N}\epsilon_k\left(\frac{\dot{x}_k}{x}+\frac{\dot{D}_k}{D_k}+i\omega\right)x_k D_k \exp(i\omega k\Delta t) \tag{11}$$

represents a noise added to the signal by the deviation from the periodic sampling rate.

Equation (10) includes only the effects of a random time distribution and does not account for random omissions or multiple values within an interval. Gaster and Roberts[6] do not address these problems, although random omissions have been analyzed by Jones.[17]

In Ref. 10, Kar, Hornkohl, and Farmer present a method for computing the spectra from Eqs. (7) and (8). Rather than using ensemble averaging, they form the sums in Eq. (7) over a long period of time and determine the spectra at selected frequencies. They show that this method yields comparable accuracy to the slotted correlation method and is superior to the periodogram approach of Gaster and Roberts.

A slotted version of Eq. (7) can also be used. Like the slotted correlation method, the random times are resolved along a grid of equidistant time intervals. Because the FFT can now be used, this method yields the fastest computation times as seen in Table 1. In Ref. 8, however, Mayo, Shay, and Riter found this estimator to yield extremely large variances in the spectra, a result confirmed in this investigation. The slotted periodogram approach is equivalent to taking the digital output from an LV system, using a digital-to-analog converter to obtain an analog signal and performing a standard discrete Fourier transform on this signal. This method for obtaining a spectrum should be used with caution.

Results and Discussion

Results are presented that evaluate the numerical efficiency and accuracy of the four methods for spectral estimation given in the last section. These estimates operate on simulated signals generated numerically using the procedure in Ref. 5, so the properties of these signals can be carefully controlled. Since the data are exact, any deviation in the resulting spectra can be attributed to the numerical procedure and not to instrument error or extraneous noise. Studies of contaminated signals have been done by Gaster and Roberts, who provide methods for minimizing a white, background noise contamination in Refs. 6 and 9. Smith and Meadows study the effects of inaccuracies in the input data in Ref. 3. In Ref. 5, Masry et al. show that aliasing is avoided when the data and randomly sampled by simulating narrow band and broadband noise signals of known spectral content.

Numerical studies of the four spectral estimates follow the test matrix in Table 2. According to Refs. 3-9, the parameters in Table 2 exert the most influence on the accuracy of spectra computed from randomly sampled data. These are the input process, type of sampling, sampling rate, the number of samples, the frequency resolution of the spectra, and the windowing. In all cases, 256 points are taken in the frequency plane. For brevity only the more significant results are presented.

Initial Tests

Initial tests were conducted using a sine wave to compare the relative accuracy and numerical efficiency between methods. Figures 1 and 2 show the results of these initial tests for a sine wave of 1000 Hz sampled at a mean sampling rate of 12,500 samples/s with a Poisson sampling time distribution. A total of 2500 points were taken, averaged over blocks of 20.48 ms duration, and multiplied by a Hanning window. Even though the input data were exact, a background noise arising from numerical error is evident in the spectra.

In Fig. 1, a comparison between the slotted correlation estimate of Smith and Meadows[3] and the exact method of Ref. 6 is made. There is a significant difference between the peak-to-noise levels obtained with these two methods, with the slotted correlation method yielding the highest signal-to-noise ratio. Because the slotted correlation is faster by a factor of $4m$, where m is the number of points in the frequency domain, the exact correlation estimate is considerably less

Table 2 Cases considered

Method	Signal[a]	Sampling data, kHz	Window	Samples
Exact correlation	Sine	12.5	Rectangular Hanning	2,500-10,000
Exact periodogram	Sine	12.5	Rectangular Hanning	2,500-10,000
Slotted correlation	Sine, narrow band, low pass	62.25-25	Rectangular Hanning	1,000-10,000
Slotted periodogram	Sine, narrow band, low pass	6.25-25	Rectangular Hanning	10,000

[a] All sine wave frequencies were 1000 Hz, all narrow band frequencies were about 1000 Hz, and low pass cutoff frequency was 1000 Hz.

efficient than the slotted approach and is eliminated from further consideration.

Comparing Fig. 1 with Fig. 2 demonstrates the superiority of the slotted correlation over the periodogram estimate from Ref. 9. Actually, the periodogram estimate is a modification of the one in Ref. 9. To attain the observed peak-to-noise ratio of 10 dB, alternating points within a given time window were taken to form a cross spectrum which is shown in Fig. 2. Without this modification, signal-to-noise ratios of only 5 dB or less are attained. New methods devised in Ref. 18 do not significantly reduce the noise levels. Regardless of the method of noise reduction in the periodogram, the slotted correlation method is not only two to four times faster, but more accurate as well.

Even though the input data are exact, numerical noise is evident in the spectra of Figs. 1 and 2. The levels are consistently higher than predicted from Eq. (4), which is derived by Gaster and Roberts[6] for the correlation estimate. The corresponding variance in the periodogram estimate is higher by a factor of 8/3 for a Hanning window.[3] According to these formulas for the variance, the estimates should yield signal-to-noise levels of over 48 dB for the given sampling rate and number of data points.

The additional variance can be explained by Eq. (4b) for the slotted correlation method and Eq. (11) for the periodogram approach. For the correlation estimate, the signal-to-noise ratio for a sine wave of angular frequency ω_0 is

$$SNR_c \simeq \frac{S_{xx}(\omega_0)}{S_{x\dot{x}e}(\omega)} \simeq \frac{1}{\omega_0\langle e\rangle}$$

where $\langle e\rangle$ is the mean square error. Assuming uniform sampling distribution over each lag interval, where H is the minimum number of products per lagged time interval,

$$\langle e\rangle = \Delta\tau/\sqrt{12H}$$

Thus the signal-to-noise ratio is 22 dB for the given test parameters, which is in agreement with the results.

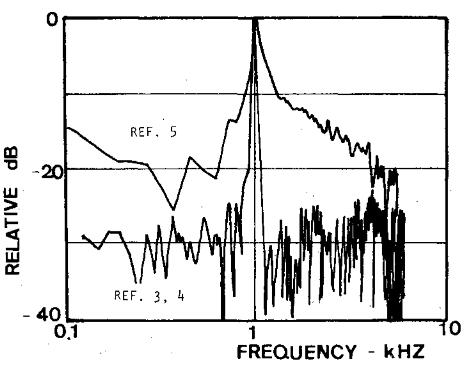

Fig. 1 Comparison of spectra obtained from correlation function-based estimates (mean sampling rate = 12,500, 2500 samples, Hanning window, sine wave at 1000 Hz).

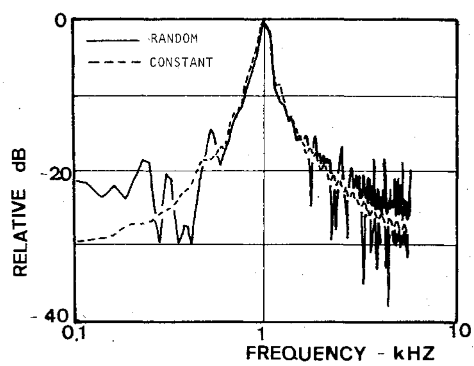

Fig. 3 Comparison of spectra computed from the correlation functions for constant and random sampling (narrow band noise, mean sampling rate = 12,500, 10,000 samples).

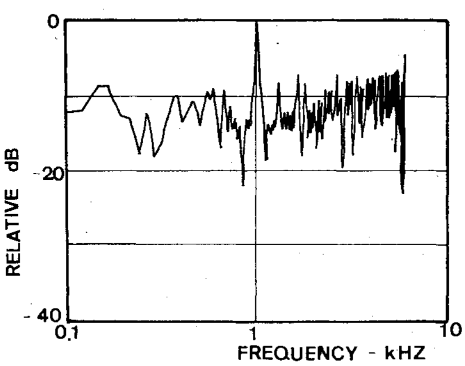

Fig. 2 Spectrum for a 1000 Hz sine wave using the periodogram estimate of Ref. 3 (mean sampling rate = 12,500, 2500 samples, Hanning window).

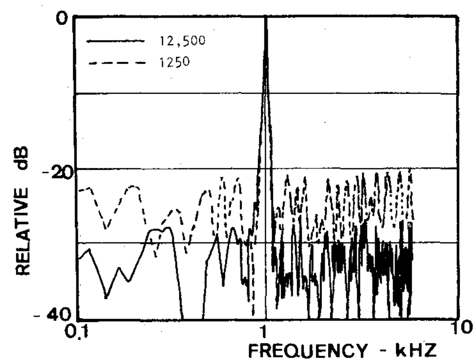

Fig. 4 Effect of sampling rate on the spectra for a 1000 Hz sine wave obtained by the slotted correlation method (Hanning window, 10,000 samples).

Similarly the periodogram signal-to-noise ratio from Eq. (11) is

$$SNR_p = \frac{1}{(\omega_0 + \omega)\langle e \rangle}$$

The deviation of e_k is roughly $\Delta t / \sqrt{12N_a}$ so

$$SNR_p \simeq \frac{\sqrt{12N_a}}{(\omega_0 + \omega)\Delta t} \sim 6 \text{ dB}$$

For $N_a = 20$, $\omega_0 = 2\pi(1000)$, $\omega = 2\pi(6250)$, $\Delta t = 80\ \mu$s.

The predicted noise exceeds the observed levels. However, the spectra in Fig. 2 are based on a modification of the spectral estimate proposed by Gaster and Roberts. Since the modified approach is essentially a cross correlation of the same signal with a different background noise, the uncorrelated noise cancels and a higher signal-to-noise ratio results than was predicted from Eq. (11).

Periodic vs Random Sampling

The contrast between the data sampled periodically and randomly are presented in Fig. 3 for the slotted correlation method. The additional variance predicted by Eq. (4b) is evident in the random sampling case and arises from the errors caused by the time approximation necessary to resolve the lagged products into equidistant slots. The corresponding spectra in Fig. 3 reflects these increased noise levels.

Equation (4a), derived by Gaster and Roberts, provides good agreement with the observed spectral variance for the periodically sampled data. In Ref. 6 they also report good agreement with spectra obtained from randomly sampled data at low sampling rates with the exact correlation estimate. However, at the high sampling rates considered here, the major source of spectral variance shifts to the nonperiodic distribution of the data in the sampling intervals. This shift also occurs in the spectra obtained from periodogram estimates.

The effects of the type of input signal on the spectrum can be seen by comparing the randomly sampled spectrum in Fig. 3 with Fig. 1. The comparison indicates comparable signal-to-noise levels predicted by Eq. (4b) for both narrow band and discrete tone signals.

Effect of Sampling Rate and Number of Samples

According to Eq. (4a) the spectral variance for the slotted correlation estimate should decrease as the sampling rate to the one-half power. Equation (4b) however is not a function of sampling rate, but depends only on the standard deviation of the mean value of the lagged products in each slot. The standard deviation, or variance, decreases as the square root of the number of samples in each slot. As shown in Fig. 4 an order-of-magnitude change in sampling rate does not appreciably alter the signal-to-noise ratio. This result is produced because, for the higher sampling rate, an order of magnitude increase in the number of points per lagged time slot occurs and reduces the noise levels by about 5 dB, as expected from Eq. (4b). Increasing the sampling rate while keeping the number of points per lagged time slot constant does not produce a significant change in signal-to-noise ratio.

Similar results are obtained from the periodogram estimates. A tenfold increase in sampling rate produces no consistent decrease in noise level, as shown in Fig. 5. Decreasing the number of averages by a factor of four increases the relative side lobe amplitude at some frequencies, although a consistent trend is not markedly evident.

Comparison of Figs. 4 and 5 indicates the correlation function produces more accurate spectral estimates than the periodogram estimate of Gaster and Roberts for a given number of samples and is also computationally faster.

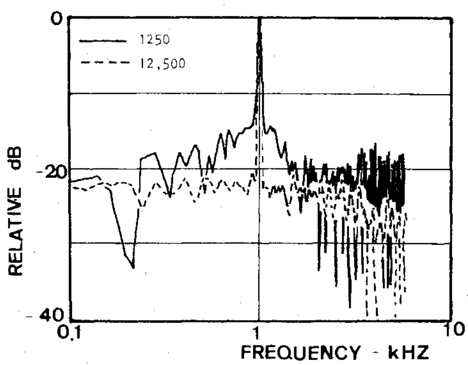

Fig. 5 Effect of increasing sampling rate on the spectra of a 1000 Hz sine wave obtained from the periodogram estimate (Hanning window, 10,000 samples).

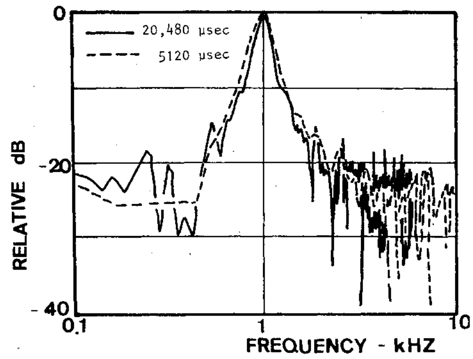

Fig. 6 Effect of increasing the sampling time interval on the spectra for narrow band noise (slotted correlation estimate, sampling rate = 12,500, Hanning window, 10,000 points).

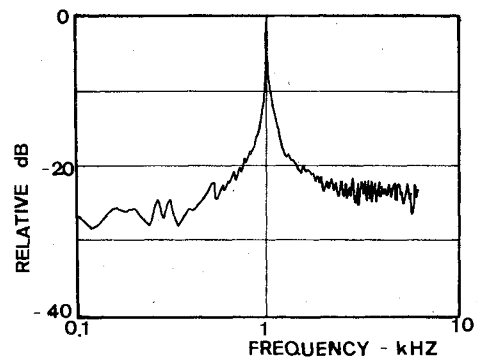

Fig. 7 Spectrum of a 1000 Hz sine wave with a rectangular window applied to the slotted correlation estimate (sampling rate = 12,500 Hz, 10,000 samples).

Sampling Interval

Increasing the sampling interval, which increases the maximum lag time for the slotted correlation estimate, decreases the signal-to-noise ratio slightly for a given number of points as shown in Fig. 6. For random sampling, this decrease occurs because the number of points per lagged time slot diminishes with decreasing maximum time lag. Thus, the variance increases according to Eq. (4b).

The same results apply to the periodogram estimate. For a given number of samples, increasing the sampling time interval increases the deviation from the corresponding periodically sampled case and decreases the number of ensemble averages obtained. These effects cause the variance to increase according to Eq. (11).

Windowing

As shown in Fig. 7, applying a rectangular window to the correlogram obtained from the slotted correlation function

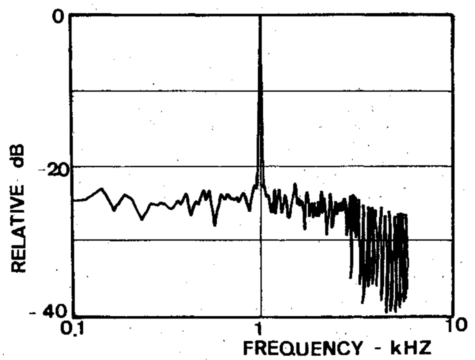

Fig. 8 Spectrum for a 1000 Hz sine wave with a rectangular window applied to the periodogram estimate (sampling rate = 12,500, 10,000 samples).

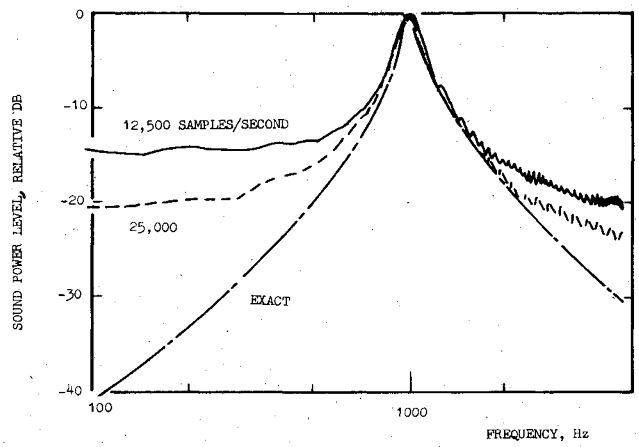

Fig. 9 Spectra obtained from slotted periodogram estimate for narrow band noise (Hanning window, 10,000 samples).

increases the noise floor by about 10 dB for randomly sampled data. Thus, while the application of a Hanning window does decrease the noise floor, the results are not as dramatic as in the periodic case.

The periodogram estimate, however, is relatively insensitive to windowing as shown in Fig. 8. In fact, compared with the spectra obtained with a Hanning window in Fig. 5, the rectangular window yields somehwat better signal-to-noise ratios.

Slotted Periodogram

Spectra computed from a modified slotted periodogram estimate were obtained based on the method presented in Ref. 11. With this method, the time domain is divided into equidistant intervals as in the slotted correlation method. If more than one point is sampled within an interval, the average value is taken. If no point is available the previous value is carried over to that interval.

As shown in Fig. 9, the accuracy of the resulting spectrum is a strong function of sampling rate. For higher sampling rates, this technique yields results of comparable accuracy to the slotted correlation method, but the computation times are reduced by a factor of about m/p, where $p = \log^2 m$. For the given cases, these computations were 30 times as fast as the slotted correlation method.

Conclusions and Recommendations

Of the four methods tested, the slotted correlation method is the best compromise between accuracy and computational efficiency. If the sampling rates are high enough, the slotted periodogram estimate is feasible and is roughly m/p times more efficient, where m is the number of samples in a given sampling interval and $p = \log^2 m$.

Compared with estimates obtained with periodically sampled data, randomly sampled data give significantly lower signal-to-noise ratios than predicted by Gaster and Roberts. This increase in noise originates from the nonuniform distribution of the data within the sampling interval. To eliminate this effect, numerical methods must be developed that do not rely on a uniform distribution of data in the sampling interval to minimize the spectral variance.

References

[1] Otnes, R. K. and Enochson, L., *Applied Time Series Analysis*: Vol. I, *Basic Techniques*, John Wiley & Sons, New York, 1978.

[2] Bendat, J. S. and Piersol, A. G., *Engineering Application of Correlation and Spectral Analysis*, John Wiley & Sons, New York, 1980, Chaps. 1 and 3.

[3] Smith, D. M. and Meadows, D. M., "Power Spectra from Random-Time Samples for Turbulence Measurements with a Laser Velocimeter," *Proceedings of the Second International Workshop on Laser Velocimetry*, Purdue University, W. Lafayette, Ind., March 1974, pp. 27-47.

[4] Mayo, W. T., "Spectrum Measurements with Laser Velocimeters," *Proceedings of Dynamic Flow Conference*, DISA Electronik A/S DK-2740, Skoolunde, Denmark, 1978.

[5] Masry, E., Klamer, D., and Mirabile, C., "Spectral Estimation of Continuous-Time Processes: Performance Comparison Between Periodic and Poisson Sampling Schemes," *IEEE Transactions on Automatic Control*, Vol. AC-23, No. 4, Aug. 1978, pp. 679-685.

[6] Gaster, M. and Roberts, J. B., "Spectral Analysis of Randomly Sampled Signals," *Journal of the Institute of Mathematics and Its Applications*, Vol. 15, 1975, pp. 195-216.

[7] Scott, P. F., "Theory and Implementation of Laser Velocimeter Turbulence Spectrum Measurements," *Proceedings of the Second International Workshop on Laser Velocimetry*, Purdue University, W. Lafayette, Ind., March 1974, pp. 47-67.

[8] Mayo, W. T., Shay, M. T., and Riter, S., "An Introduction to the Estimation of Power Spectra from Single Particle LV Data," *Proceedings of the LDA Workshop*, Oklahoma State University, Stillwater, June 1973.

[9] Gaster, M. and Roberts, J. B., "Spectral Analysis of Randomly Sampled Records by a Direct Transform," *Proceedings of the Royal Society of London*, Ser. A, Vol. 354, 1977, pp. 27-58.

[10] Kar, M. L., Hornkohl, J. O., and Farmer, W. M., "An Algorithm for Spectral Estimation of Randomly Sampled Data," *Proceedings of Southeastcon '81*, Huntsville, Ala., 1981.

[11] Starner, S. H. and Bilger, R. W., "Measurements of Velocity and Concentration in Turbulent Diffusion Flames with Pressure Gradients," AIAA Paper 80-0205, Jan. 1980.

[12] Buchhave, P., "Errors and Correction Methods in Turbulence Measurements with an LDA," Ph.D. Thesis, State University of New York, Buffalo, N.Y., 1979.

[13] Buchhave, P., George, W. K., and Lumley, J. L., "The Measurement of Turbulence with the Laser Doppler Anemometer," *Annual Review of Fluid Mechanics*, Vol. 11, 1979, pp. 443-503.

[14] Whiffen, M. C., "Polar Response of an LV Measurement Volume," *Proceedings of the Minnesota Symposium on Laser Anemometry*, Univ. of Minnesota, Bloomington, Minn., 1975, pp. 589-590.

[15] Oppenheim, A. V. and Schafer, R. W., *Digital Signal Processing*, Prentice-Hall, Englewood, N.J., 1975, Chaps. 6 and 11.

[16] Jones, R. H., "Aliasing with Unequally Spaced Observations," *Journal of Applied Meteorology*, Vol. 11, No. 2, 1972, pp. 245-254.

[17] Jones, R. H., "Spectral Estimation with Missing Observations," *Annals of the Institute of Statistical Mathematics*, Vol. 23, 1971, pp. 387-398.

[18] Roberts, J. B., Downie, J., and Gaster, M., "Spectral Analysis of Signals from a Laser Doppler Anemometer Operating in the Burst Mode," *Journal of Physics E: Scientific Instruments*, Vol. 13, 1980, pp. 977-981.